Materials Science & Engineering A 597 (2014) 70–74

Contents lists available at ScienceDirect

Materials Science & Engineering A

journal homepage: www.elsevier.com/locate/msea

A novel Ni_2AlTi-containing composite with excellent wear resistance and anomalous flexural strength

H. Zhang [a,b], X.H. Wang [a], Z.J. Li [a,b], M.Y. Liu [a], Y.C. Zhou [a,c,*]

[a] Shenyang National Laboratory for Materials Science, Institute of Metal Research, Chinese Academy of Sciences, 72 Wenhua Road, Shenyang 110016, China
[b] University of Chinese Academy of Sciences, Beijing 100049, China
[c] Science and Technology of Advanced Functional Composite Laboratory, ARIMPT, No. 1 South Dahongmen Road, Beijing 100076, China

ARTICLE INFO

Article history:
Received 20 October 2013
Received in revised form
17 December 2013
Accepted 17 December 2013
Available online 27 December 2013

Keywords:
Carbides
Twins
Composites
Flexural strength anomaly
Ti_3AlC_2

ABSTRACTS

A novel twinning platelets strengthened TiC–Ni_2AlTi composite was designed and fabricated by an *in situ* reactive hot-pressing method of blended Ti_3AlC_2 and Ni powders. Upon de-intercalation of Al from nanolaminated Ti_3AlC_2 upon heating, TiC twinning platelets with width in submicrometer size were introduced. The obtained composite exhibits excellent wear resistance, high flexural strength, moderate fracture toughness and Vickers hardness. Unexpectedly, the flexural strength of the composite increases with temperature rising from 500 to 800 °C, reaching a maximum of 936 MPa at 800 °C, thereby benefiting the application as cutting tools.

1. Introduction

Being hard and wear resistant, cemented carbides that combine the strength of the carbides and the ductility of binders represent extensive industrial implementations, including cutting tools, drilling bits, wire drawing dies, punch sets, etc. [1]. In these materials, expensive cobalt is widely used as the binder due to its unique combination of properties. However, the cobalt cemented carbides show unsatisfied corrosion resistance in aqueous and acidic environments [1]. To improve the corrosion resistance and replace costly Co, a large number of ductile metals and intermetallics have been intensively investigated as inexpensive binders [1–5]. It is well established that intermetallics cemented titanium carbides are superior to WC/Co in terms of high-temperature mechanical performance and density [1,6,7]. Ni_2AlTi exhibits higher creep strength than NiAl [8–10], lower density than Ni_3Al and comparable oxidation resistance to NiAl [11], and thus is a promising binder to produce TiC cement for high temperature applications. However, cemented TiC using Ni_2AlTi as the binder has rarely been studied so far.

It is well acknowledged that the mechanical properties of cemented carbides are determined not only by the component phases, but also by the microstructures. In order to improve the mechanical performance of TiC and TiC-containing composites, the size and morphology of TiC grains must be controlled to tailor their mechanical properties [12–16]. As a new way to improve the strength and hardness of metals and ceramics [17,18], introducing nanotwins in the TiC-containing composite is the target of many material designs, and has been attempted by several groups [19–22]. Unfortunately, this target has not been reached due to the extremely high twin boundary energy of pure TiC [23,24]. Recent investigations on the thermal stability of layered ternary carbides and nitrides (MAX phases) demonstrate that high density TiC microtwins can be formed when these carbides (like Ti_3AlC_2,Ti_3SiC_2 and Ti_2SnC) are heat treated in the powder bed or embedded in some metals [19,23,25,26]. The mechanism that underpins the formation of TiC twins is the anisotropic chemical bonding in these layered ternary carbides. For example in Ti_3AlC_2, the Ti–Al bonds are much weaker than the Ti–C bonds, and Al atoms are consequently prone to de-intercalation under critical circumstances [19,23,27,28]. The de-intercalation of Al atoms results in the formation of TiC twins in nanoscale [19,23]. Such de-intercalation of Al from Ti_3AlC_2 and the formation of TiC twins in metals like Cu and Ni shed new light on introducing TiC twins in the microstructure design of new TiC–Ni_2AlTi composite.

In this work, introducing TiC twinning platelets was achieved by *in situ* reaction using Ti_3AlC_2 and Ni powders as starting materials. The formed new composite exhibits excellent wear resistance, high flexural strength, moderate fracture toughness and Vickers hardness. In addition, anomalous high temperature strength, *i.e.*, the flexural strength increases with temperature from 500 to 800 °C, was observed for the first time in Ni_2AlTi-containing materials.

* Corresponding author at: Science and Technology of Advanced Functional Composite Laboratory, ARIMPT, No.1 South Dahongmen Road, Beijing 100076, China. Tel.: +86 10 68382478; fax: +86 10 68759874.
E-mail address: yczhou714@gmail.com (Y.C. Zhou).

0921-5093/$ - see front matter © 2013 Elsevier B.V. All rights reserved.
http://dx.doi.org/10.1016/j.msea.2013.12.066

2. Experimental method

Fully dense TiC–Ni_2AlTi composite was prepared by reactive hot-pressing of nanolaminated Ti_3AlC_2 (−300 mesh) and Ni (−300 mesh, Sinopharm Chemical Reagent Co., Ltd.) powders. The Ti_3AlC_2 powder was synthesized using the method reported previously [29]. To prepare the TiC–Ni_2AlTi composite, Ti_3AlC_2 and Ni powders with a molar ratio of 1:2 were mixed with absolute ethanol and agate balls in an agate jar for 12 h, and followed by drying at 60 °C for 10 h. The homogenized powders were uniaxially pressed into a green compact in a graphite mold with an inner diameter of 50 mm. After that, the green compact, together with the mold, was put into a hot-pressing furnace and heated, respectively, up to the target temperatures of 750 °C, 850 °C, 1000 °C, 1200 °C and 1350 °C at a heating rate of 10 °C/min in a flowing Ar atmosphere, then held for 1 h under a pressure of 30 MPa. Subsequently, the sample was naturally cooled down to room temperature in the furnace. For comparative purpose, pure Ni_2AlTi was prepared following the similar procedure at 1200 °C.

The density of the bulk sample was determined by the Archimedes method. X-ray diffraction (XRD) pattern was collected in an X-ray diffractometer (Rigaku D/max-2400, Tokyo, Japan) with Cu $K\alpha$ radiation. The microstructural characterizations were performed using a scanning electron microscope (SEM, LEO, SUPRA35, Ammerbuch, Germany) and a transmission electron microscope (TEM, FEI Tecnai G^2 F20) working at 200 kV. The thin film sample for TEM observation was prepared by slicing, grinding, dimpling and Ar-ion-milling. The fracture toughness (K_{IC}) was determined by three-point bending test with the single-edge notched beam (SENB) method at a crosshead speed of 0.05 mm/min, the sample dimension being 4 mm × 8 mm × 36 mm. A notch of 4 mm in length and 0.15 mm in width was made by the electrical discharge method. The sliding wear tests were carried out on a microtribometer (UMT-2, CETR, Campbell, *CA*) at a load of 20 N. Commercially available AISI52100 steel balls (HRc 62–63, Ra 0.10 μm) and Si_3N_4 balls (Hv 14–16 GPa, Ra 0.10 μm) with a diameter of 4.76 mm were used as counter materials. The Vickers microhardness was measured at loads of 3, 10, 30, 50 and 100 N with a dwell time of 15 s. The flexural strength was measured by the three-point bending test using samples with a dimension of 3 mm × 4 mm × 36 mm, with the span being 30 mm and the crosshead speed being 0.5 mm/min. The flexural strength was measured at room temperature, 500 °C, 700 °C, 800 °C and 900 °C, respectively. At each temperature, six specimens were tested.

3. Results

The Ni–Al–Ti ternary phase diagram shows that Ni_2AlTi can be formed at as low as 750 °C. Thus the composite was sintered at 750 °C, 850 °C, 1000 °C and 1200 °C, to determine a suitable preparation temperature. Fig. 1 shows the XRD pattern of the composite prepared at different temperatures. It is clear that TiC and Al_3Ni (the signature peak is 2θ=45.9°) formed at 750 °C as a result of the reaction of Ni and de-intercalated Al. At 850 °C, TiC and Ni_3Al (the signature peak is 2θ=24.8°) were identified. As more Al de-intercalated and reacted with Ni, NiAl formed at 1000 °C. Besides, partial Ti diffused out of the Ti_3C_2 nanoslabs and reacted with Ni_3Al and NiAl, forming some amounts of Ni_2AlTi. At 1200 °C, all the Ni was exhausted and formed Ni_2AlTi and TiC. The nominal reaction equation could be described as $Ti_3AlC_2+2Ni=Ni_2AlTi+2TiC$. To obtain a fully dense bulk sample, the hot-pressing temperature was finally raised up to 1350 °C.

Fig. 2 compares the XRD patterns of the dense TiC–Ni_2AlTi composite and Ni_2AlTi. All the main peaks can be indexed to TiC and Ni_2AlTi. The peak at 2θ=44° has an obvious shoulder, marked

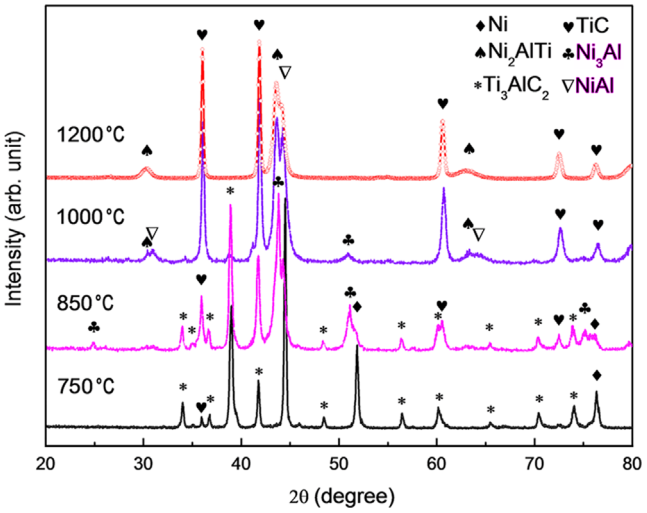

Fig. 1. XRD patterns of samples sintered at 750, 850, 1000 and 1200 °C.

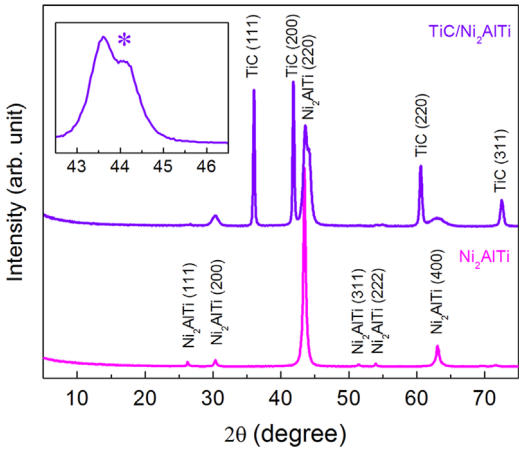

Fig. 2. XRD patterns of TiC–Ni_2AlTi composite and Ni_2AlTi. The inset shows the peak splitting of the composite.

with an asterisk in the inset, which is due to the peak overlap of Ni_2AlTi (220) and NiAl (110). The remaining NiAl and Ni_2AlTi forms a so-called Widmanstätten-type structure (or maze structure) [9,30], as shown in Fig. 3(a). Because of the maze structure, the peaks belonging to Ni_2AlTi are somewhat broader than that of pure Ni_2AlTi (the lower curve in Fig. 2). For example, the full width of half maximum of the (200) peak belonging to Ni_2AlTi of the composites is 1.01°, whereas that of pure Ni_2AlTi is only 0.48°. As shown by the typical SEM image in Fig. 3(b), the as-prepared composite with a density of 5.57 g/cm^3 is fully dense. Careful analysis of the microstructure demonstrates that TiC twining laminas were successfully introduced, as labeled by the arrows in Fig. 3(c). The twinning laminas have a dimension of about 200 nm in width and 2–3 μm in length. Fig. 3(d) presents a high resolution transmission electron microscopy (HRTEM) image of TiC twinning platelets. Different from the model proposed by Zhang et al. [23], the Σ3 {111} twin boundary is coherent. The two parts at both sides of the twin boundary are ideally mirror-symmetric. The width of the TiC twinning platelets is very small (~300 nm), resulting in an increase in the amount of coherent twin boundaries (CTBs), which partially contributes to the high strength of the composites, as is stated in the following.

Fig. 4(a) shows the load dependence of Vickers hardness. Insets present the optical photographs of indents. The Vickers hardness of the synthesized composite is about 10 GPa (at a load of 100 N). The indent at the load of 50 N shares the feature of metals, with no cracks

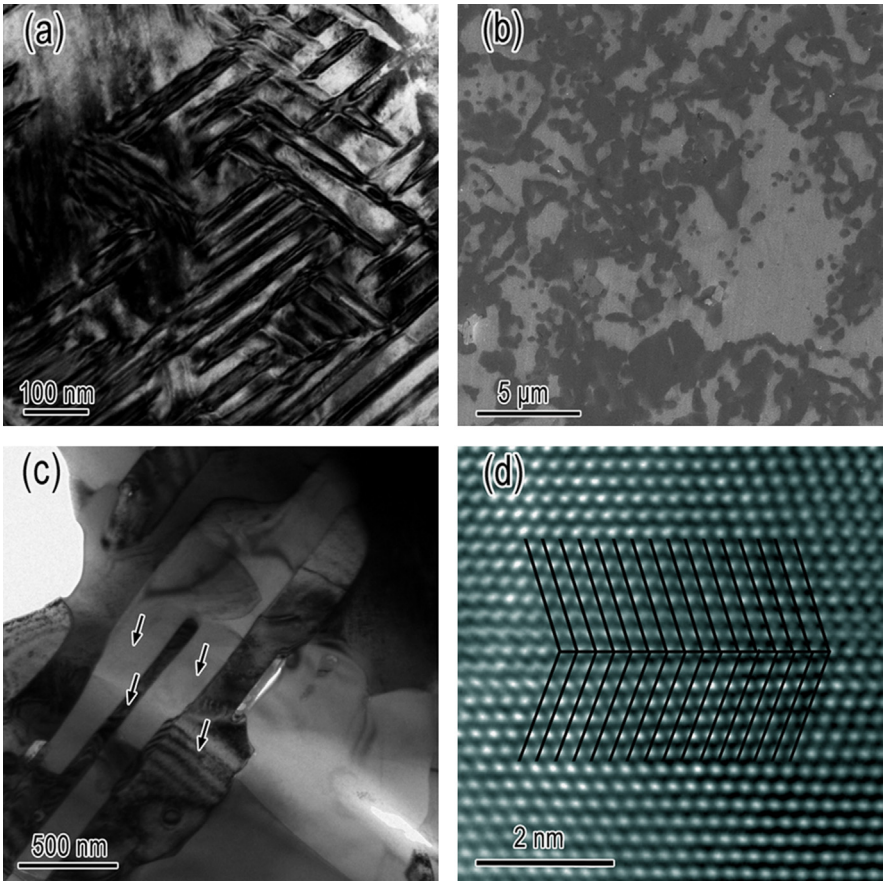

Fig. 3. (a) TEM bright field image of maze structure of NiAl and Ni_2AlTi; (b) typical SEM image of the as-prepared sample; (c) TEM bright field image of TiC twinning laminas, with the twins being marked with arrows; (d) HRTEM image of TiC twin boundary.

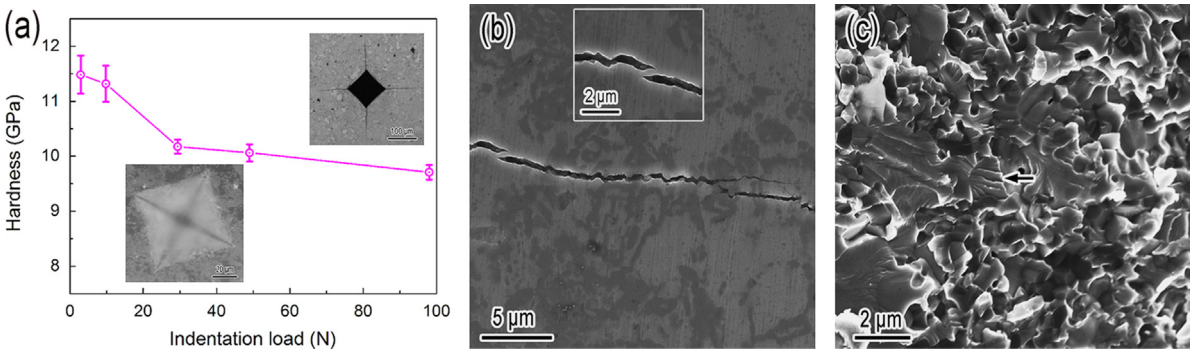

Fig. 4. (a) Load dependence of Vickers hardness. The insets show indent morphology under 50 (lower) and 100 N (upper), respectively. SEM image of (b) crack initiated at the corner of the indent, the inset highlights the bridging effect, and (c) fracture morphology.

initiated. As the load increases to 100 N, cracks initiated at the corner of the indentation. The details of the cracks are highlighted in Fig. 4(b), in which crack deflection and crack bridging are visible. The indentation morphology and crack characteristics indicate that the composite is tolerant to indentation damage. In agreement with the microstructural observation, the TiC–Ni_2AlTi composite has a fracture toughness of 5.0 MPa $m^{1/2}$. A typical fracture surface is presented in Fig. 4(c), wherein the cleavage step marked with arrows can be clearly seen, *i.e.*, transgranular fracture prevails. The predominance of transgranular fracture indicates that the TiC/Ni_2AlTi interface is strong, which has been verified through interface microstructural observation by HRTEM. The HRTEM image of the TiC/Ni_2AlTi interface and the corresponding fast Fourier transformation (FFT) pattern is presented in Fig. 5(a) and (b), respectively. The orientation relationship is (220) Ni_2AlTi||(111) TiC, $[1\bar{1}0]$ Ni_2AlTi||$[1\bar{1}0]$ TiC. The diffraction spots circled in Fig. 5(b) were used to reconstruct an inverse FFT image. As shown in Fig. 5(c), the TiC/Ni_2AlTi interface is semi-coherent, with misfit dislocations marked with inclined "T". The semi-coherent interface contributes to a strong TiC/Ni_2AlTi interface.

Due to the strong interfaces, the as-synthesized TiC–Ni_2AlTi composite has novel wear resistance; the specific wear rate against Si_3N_4 balls at the load of 20 N is as low as 2.2×10^{-9} cm^3/mN. When tested against AISI52100 steel balls under the identical condition, the wear rate of the composite is undetectable within the resolution (0.01 mg) of the balance used for measuring the mass change before and after the wear test.

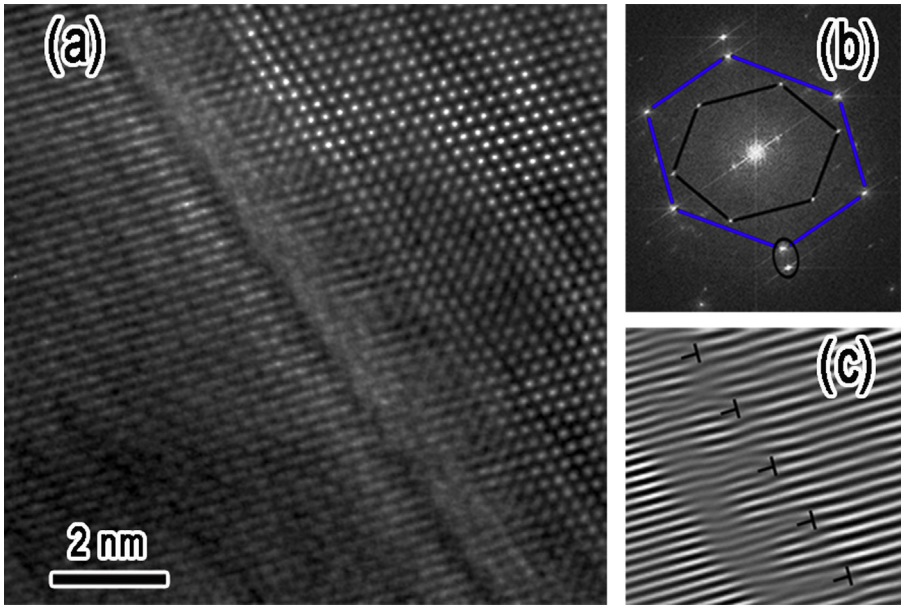

Fig. 5. (a) HRTEM image of the Ni_2AlTi/TiC interface. (b) FFT pattern of (a), the diffraction spots linked by dark lines and blue lines belong to Ni_2AlTi and TiC, respectively. (c) Inverse FFT image by masking the circled diffraction spots in (b), the misfit dislocations are illustrated by the inclined letter T.

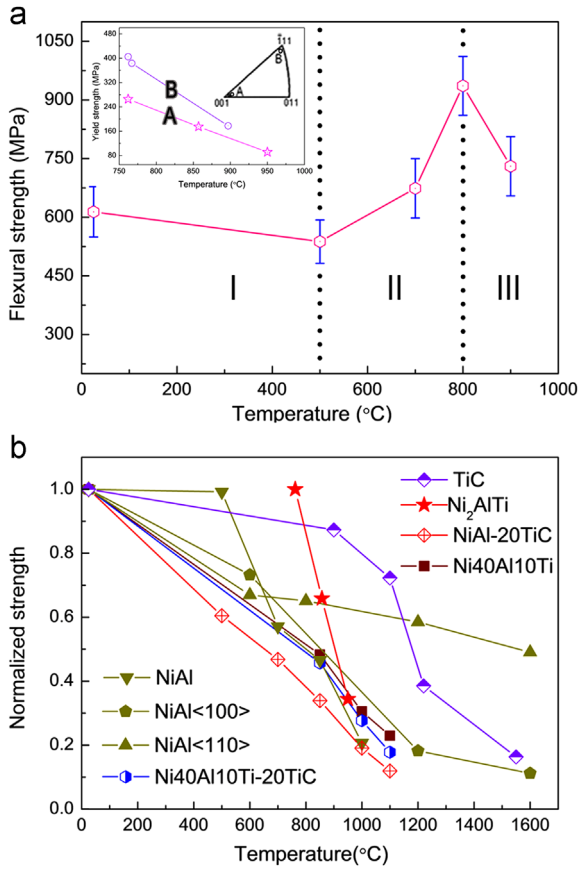

Fig. 6. (a) Temperature dependence of flexural strength, showing three distinct regions. The inset shows the dependence of the yield strength of Ni_2AlTi single crystal on temperature, the data was adapted from reference [10]. (b) Temperature dependence of normalized strength (normalized by the max strength) of TiC, NiAl, Ni_2AlTi and selective corresponding composites; the data was adapted from [10,35–37].

Flexural strengths of the TiC/Ni_2AlTi composite at ambient and elevated temperatures were evaluated by three-point bending tests in air. Fig. 6(a) presents the temperature dependence of flexural strength. It can be distinctively divided into three temperature regions. In region I, the flexural strength decreases with temperature. In region II, the flexural strength unexpectedly increases with temperature increase, indicating a phenomenon of flexural strength anomaly (FSA). The strength reaches a maximum of 936 MPa at 800 °C, being 1.7 times of the minimum and 50% higher than that at room temperature. In region III, the flexural strength decreases again but more rapidly with the increase in temperature.

4. Discussion

The pull-out of the hard ceramic particles is one of the causes for severe wear of ceramic/metal composites [31,32]. The semi-coherent TiC/Ni_2AlTi interface in this work can strengthen the hetero-phase boundary between TiC and Ni_2AlTi. In addition, TiC is subjected to compressive stress ($\delta = 2((d_{220}^{Ni_2AlTi} - d_{111}^{TiC})/(d_{220}^{Ni_2AlTi} + d_{111}^{TiC})) = -18.66\%$) when the TiC and Ni_2AlTi grains are aligned as the orientation relationship as presented in Fig. 5(b). The residual compressive stress in TiC can suppress the crack initiation within the interface. Both the strengthened TiC/Ni_2AlTi hetero-phase interface and residual compressive stress in TiC can hinder the pull-out of TiC, and thus play a positive and beneficial role on wear performance. The specific wear rate against Si_3N_4 balls at the load of 20 N, 2.2×10^{-9} m^3/mN is slightly lower than, but still comparable to, other TiC-based and WC-based cermets [6,33] and is 1–2 orders of magnitude lower than that of the Si_3N_4–graphene, Si_3N_4–CNT composites [34]. Since only one composition of TiC/Ni_2AlTi composite was designed in the present study, the results are quite preliminary and there is a huge space to modulate the wear performance by optimizing the amount of the binder, Ni_2AlTi.

The flexural strength of TiC/Ni_2AlTi shows a positive temperature dependence (500–800 °C), namely, the flexural strength increases with increase in temperature. Similar to the yield strength anomaly (YSA) in intermetallics with $L1_2$ structure, the flexural strength anomaly in this study is abbreviated to FSA. The FSA in this work is surprising, because neither the yield strength of monolithic TiC, Ni_2AlTi or NiAl [10,35–37], nor the

strength of 20 wt%TiC–NiAl–Ni_2AlTi composite [36] increase with temperature increase, as shown in Fig. 6(b). The knowledge of the observed FSA is quite limited at present. Since the rupture strength of the composite is over the yield strength of Ni_2AlTi, as demonstrated in the inset of Fig. 6(a), it is likely that the FSA is caused by the unique, not well understood plastic deformation of Ni_2AlTi. A detailed investigation is in progress in the authors' laboratory. From an industrial point of view, the increased strength in temperature range 500–800 °C is much beneficial for the application as cutting tools, whose max temperature can reach 600–800 °C without water cooling during cutting.

The results reported herein were based on the TiC–Ni_2AlTi composite with a nominal molar ratio of 2:1, which should be quite preliminary. Further improvement on the tribological and mechanical performances of TiC–Ni_2AlTi composite is reasonably expected by means of composition optimization. In addition, the starting material used in the present study, Ti_3AlC_2, belongs to a big family of layered ternary carbides. In the family, there are over 60 structurally-related members with similar bonding properties [38]. Thus the strategy proposed in this paper is applicable to produce new generation TiC-based cements with positive dependence of flexural strength on temperature. For example, Ti(C,N) cermet is competitive to WC/Co hardmetals on an industrial scale [7,39,40]. It should be emphasized that more work to optimize the composition, for example, replace the Ti_3AlC_2 using $Ti_3Al(C,N)_2$ as starting material, is needed.

5. Conclusions

In summary, with the strengthening of TiC CTBs and semi-coherent TiC/Ni_2AlTi interface, a new TiC–Ni_2AlTi composite with the combination of excellent wear resistance, high flexural strength, moderate fracture toughness and Vickers hardness was synthesized for the first time by the *in situ* reaction between Ti_3AlC_2 and Ni powders. The flexural strength increases with the temperature rising from 500 to 800 °C, reaching a maximum of 936 MPa at 800 °C.

Acknowledgments

This work was supported by the Chinese Academy of Sciences and the IMR Innovative Research Foundation. X.H. Wang gratefully acknowledges the support of K.C. Wang Education Foundation, Hong Kong.

References

[1] K.P. Plucknett, T.N. Tiegs, P.F. Becher, S.B. Waters, P.A. Menchhofer, in: J.B. Wachtman (Ed.), Proceedings of the 20th Annual Conference on Composites, Advanced Ceramics, Materials, and Structures—A: Ceramic Engineering and Science Proceedings, John Wiley & Sons, Inc., 2008, pp. 314–321.
[2] W. Hua, X. Wu, D. Shen, H. Lu, M. Polak, Intermetallics 11 (2003) 981–985.
[3] K.P. Plucknett, P.F. Becher, R. Subramanian, J. Mater. Res. 12 (1997) 2515–2517.
[4] J. Wall, H. Choo, T.N. Tiegs, P.K. Liaw, Mater. Sci. Eng. A 421 (2006) 40–45.
[5] H.E. Exner, Int. Mater. Rev. 24 (1979) 149–173.
[6] S. Buchholz, Z.N. Farhat, G.J. Kipouros, K.P. Plucknett, Can. Metall. Q. 52 (2013) 69–80.
[7] S. Park, S. Kang, Scr. Mater. 52 (2005) 129–133.
[8] P. Strutt, R. Polvani, J. Ingram, Metall. Mater. Trans. A 7 (1976) 23–31.
[9] R. Yang, J.A. Leake, R.W. Cahn, J. Mater. Res. 6 (1991) 343–354.
[10] M. Yamaguchi, Y. Umakoshi, T. Yamane, Philos. Mag. A 50 (1985) 205–220.
[11] C. Lee, P. Shen, J. Mater. Sci. 24 (1989) 3707–3711.
[12] S.D. Luo, Q. Li, J. Tian, C. Wang, M. Yan, G.B. Schaffer, M. Qian, Scr. Mater. 69 (2013) 29–32.
[13] S. HSU, M. Meyers, A. Berkowitz, Scr. Metall. Mater. 32 (1995) 805–808.
[14] D. Gu, G. Meng, C. Li, W. Meiners, R. Poprawe, Scr. Mater. 67 (2012) 185–188.
[15] M. Sherif El-Eskandarany, J. Alloys Compd. 305 (2000) 225–238.
[16] A. Sen, T. Kar, S.K. Pradhan, J. Alloys Compd. 557 (2013) 47–52.
[17] K. Lu, Science 328 (2010) 319–320.
[18] Y. Tian, B. Xu, D. Yu, Y. Ma, Y. Wang, Y. Jiang, W. Hu, C. Tang, Y. Gao, K. Luo, Z. Zhao, L.M. Wang, B. Wen, J. He, Z. Liu, Nature 493 (2013) 385–388.
[19] J. Zhang, Y.C. Zhou, J. Mater. Res. 23 (2008) 924–932.
[20] R. Yu, Q. Zhan, L.L. He, Y.C. Zhou, H.Q. Ye, Acta Mater. 50 (2002) 4127–4135.
[21] R. Yu, L.L. He, H.Q. Ye, Acta Mater. 51 (2003) 2477–2484.
[22] W.T. Hu, S.C. Liu, B. Wen, J.Y. Xiang, F.S. Wen, B. Xu, J.L. He, D.L. Yu, Y.J. Tian, Z.Y. Liu, J. Appl. Crystallogr. 46 (2013) 43–47.
[23] J. Zhang, J.Y. Wang, Y.C. Zhou, Acta Mater. 55 (2007) 4381–4390.
[24] B.J. Kooi, M. Kabel, A.B. Kloosterman, J.T.M. De Hosson, Acta Mater. 47 (1999) 3105–3116.
[25] J. Emmerlich, D. Music, P. Eklund, O. Wilhelmsson, U. Jansson, J.M. Schneider, H. Hogberg, L. Hultman, Acta Mater. 55 (2007) 1479–1488.
[26] J.Y. Wu, Y.C. Zhou, J.Y. Wang, W. Wang, C.K. Yan, Z. Metallkd. 96 (2005) 1314–1320.
[27] J. Xie, X.H. Wang, A.J. Li, F.Z. Li, Y.C. Zhou, Corros. Sci. 60 (2012) 129–135.
[28] X.H. Wang, Y.C. Zhou, J. Mater. Sci. Technol. 26 (2010) 385–416.
[29] X.H. Wang, Y.C. Zhou, Acta Mater. 50 (2002) 3141–3149.
[30] J.D. Whittenberger, R.K. Viswanadham, S.K. Mannan, K.S. Kumar, J. Mater. Res. 4 (1989) 1164–1171.
[31] G.Y. Lee, C.K.H. Dharan, R.O. Ritchie, Wear 252 (2002) 322–331.
[32] W. Simm, S. Freti, Wear 129 (1989) 105–121.
[33] C.C. Onuoha, G.J. Kipouros, Z.N. Farhat, K.P. Plucknett, Wear 303 (2013) 321–333.
[34] P. Hvizdoš, J. Dusza, C. Balázsi, J. Eur. Ceram. Soc. 33 (2013) 2359–2364.
[35] G. Das, K.S. Mazdiyasni, H.A. Lipsitt, J. Am. Ceram. Soc. 65 (1982) 104–110.
[36] D.T. Jiang, J.T. Guo, C.X. Shi, D.L. Lin, J. Mater. Sci. Lett. 19 (2000) 115–117.
[37] R. Darolia, J. Miner. Met. Mater. Soc. 43 (1991) 44–49.
[38] M.W. Barsoum, M. Radovic, Annu. Rev. Mater. Res. 41 (2011) 195–227.
[39] P. Ettmayer, Annu. Rev. Mater. Sci. 19 (1989) 145–164.
[40] P. Ettmayer, H. Kolaska, W. Lengauer, K. Dreyer, Int. J. Refract. Met. Hard Mater. 13 (1995) 343–351.